

SECONDARY CIRCULATION IN GRANULAR FLOW THROUGH NONAXISYMMETRIC HOPPERS

PIERRE A. GREMAUD*, JOHN V. MATTHEWS†, AND DAVID G. SCHAEFFER‡

Abstract. Jenike’s radial solution, widely used in the design of materials-handling equipment, is a similarity solution of steady-state continuum equations for the flow under gravity of granular material through an infinite, right-circular cone. In this paper we study how the geometry of the hopper influences this solution. Using perturbation theory, we compute a first-order correction to the (steady-state) velocity resulting from a small change in hopper geometry, either distortion of the cross section or tilting away from vertical. Unlike for the Jenike solution, all three components of the correction velocity are nonzero: i.e., there is secondary circulation in the perturbed flow. We show that, depending on hopper and material parameters, the perturbed velocity depends sensitively, to an astonishing degree, on hopper geometry. These results suggest that, even in a vertical conical hopper, solutions with circulation may bifurcate from the Jenike solution, a phenomenon to be investigated in a future paper.

Key words. granular, similarity solution, perturbation theory

AMS subject classifications. 65L80, 35J65, 76T25

1. Introduction. In manufacturing industries, raw materials are stored in granular form in a silo, and when needed, they are expected to flow out of the silo under gravity through a hopper. Problems in the discharge process are frequent and expensive, see e.g. [9]. As demonstrated by a Rand Corporation study [10], these problems are symptomatic of our poor understanding of the behavior of granular materials¹.

Jenike’s radial solution is a central component of silo design. Despite its importance, this solution is subject to many severe restrictions:

1. Granular material is modeled as a continuum, with an *ad hoc* constitutive law.
2. The flow is assumed to be steady.
3. The flow domain, a mathematical idealization, is an infinite cone, given in spherical polar coordinates by the formula

$$\{(r, \theta, \phi) : 0 < r < \infty, 0 \leq \theta < \theta_w\}, \quad (\theta_w = \text{constant}).$$

4. Only similarity solutions are considered.

*Department of Mathematics and Center for Research in Scientific Computation, North Carolina State University, Raleigh, NC 27695-8205, USA (gremaud@math.ncsu.edu). Partially supported by the Army Research Office (ARO) through grant DAAD19-99-1-0188 and by the National Science Foundation (NSF) through grant DMS-9818900.

†Department of Mathematics, Duke University, Durham, NC 27708-0320, USA (jvmatthe@math.duke.edu). Partially supported by the National Science Foundation through grant DMS-9983320

‡Department of Mathematics & Center for Nonlinear and Complex Systems, Duke University, Durham, NC 27708-0320, USA (dgs@math.duke.edu). Partially supported by the National Science Foundation through grant DMS-9803305

¹The study compared the design output and the actual output of a total of 60 manufacturing plants in various industries, 22 that were based primarily on liquids-processing technology and 38 on solids-processing technology. On average, the liquids-processing plants produced at 84% of design capacity while the solids-processing plants produced at only 63% of design capacity. To quote Merrow, “In economic terms, the difference between 63% of design and 84% is very large. It implies a capital cost per unit of output about one-third higher for the solids-processing plants, on the basis of poor performance alone. In addition, poor performance is inevitably associated with higher operating and maintenance costs per unit of product.” Moreover, the standard deviation of the solids-processing data set was much greater, indicative of our difficulties in predicting the behavior of granular solids.

Report Documentation Page				Form Approved OMB No. 0704-0188	
Public reporting burden for the collection of information is estimated to average 1 hour per response, including the time for reviewing instructions, searching existing data sources, gathering and maintaining the data needed, and completing and reviewing the collection of information. Send comments regarding this burden estimate or any other aspect of this collection of information, including suggestions for reducing this burden, to Washington Headquarters Services, Directorate for Information Operations and Reports, 1215 Jefferson Davis Highway, Suite 1204, Arlington VA 22202-4302. Respondents should be aware that notwithstanding any other provision of law, no person shall be subject to a penalty for failing to comply with a collection of information if it does not display a currently valid OMB control number.					
1. REPORT DATE 2002		2. REPORT TYPE		3. DATES COVERED 00-00-2002 to 00-00-2002	
4. TITLE AND SUBTITLE Secondary Circulation in Granular Flow Through Nonaxisymmetric Hoppers				5a. CONTRACT NUMBER	
				5b. GRANT NUMBER	
				5c. PROGRAM ELEMENT NUMBER	
6. AUTHOR(S)				5d. PROJECT NUMBER	
				5e. TASK NUMBER	
				5f. WORK UNIT NUMBER	
7. PERFORMING ORGANIZATION NAME(S) AND ADDRESS(ES) North Carolina State University, Center for Research in Scientific Computation, Raleigh, NC, 27695-8205				8. PERFORMING ORGANIZATION REPORT NUMBER	
9. SPONSORING/MONITORING AGENCY NAME(S) AND ADDRESS(ES)				10. SPONSOR/MONITOR'S ACRONYM(S)	
				11. SPONSOR/MONITOR'S REPORT NUMBER(S)	
12. DISTRIBUTION/AVAILABILITY STATEMENT Approved for public release; distribution unlimited					
13. SUPPLEMENTARY NOTES The original document contains color images.					
14. ABSTRACT see report					
15. SUBJECT TERMS					
16. SECURITY CLASSIFICATION OF:			17. LIMITATION OF ABSTRACT	18. NUMBER OF PAGES 20	19a. NAME OF RESPONSIBLE PERSON
a. REPORT unclassified	b. ABSTRACT unclassified	c. THIS PAGE unclassified			

In this paper we relax restrictions 3 and 4 partly. Specifically, we generalize the domain to an infinite *pyramidal* hopper described by the inequality

$$(1.1) \quad 0 \leq \theta < \theta_w + \epsilon \cos m\phi,$$

where ϵ is a small parameter and m is a positive integer. Assuming a perturbation series

$$v^{(0)} + \epsilon v^{(1)} + \dots$$

for the flow velocity in the domain (1.1), where $v^{(0)}$ is Jenike's solution, we derive a linear PDE for the first-order correction $v^{(1)}$. The r -dependence of $v^{(1)}$ still has similarity form, and the ϕ -dependence may be handled by separation of variables. In this way we reduce solving the PDE for $v^{(1)}$ to solving a two-point boundary problem on the interval $0 < \theta < \theta_w$.

In Jenike's solution, only the radial component $v_r^{(0)}$ of the velocity is nonzero. By contrast, all three components of the correction velocity $v^{(1)}$ are nonzero. In other words, *distortion of the conical domain leads to secondary circulation*. For example, in Figure 5.1 below, the flow in the θ, ϕ -directions is shown in two cases which correspond to a circular hopper that is tilted slightly to the right, and in Figure 5.2, in two cases which correspond to a slightly distorted vertical hopper.

The boundary problem for $v^{(1)}$ contains three significant parameters: the angle of internal friction δ , the coefficient of wall friction μ_w , and the opening angle of the hopper θ_w . (The subscript w is mnemonic for *wall*.) Surprising behavior occurs when these parameters are varied. In the first place, the direction of circulation may reverse itself. This is illustrated for instance by Figure 5.2: δ and θ_w are the same for both parts of the figure, but μ_w is larger in the bottom part. As illustrated in Figure 5.1, the topology of the circulation may change as μ_w varies. Most surprising of all, the circulation does not reverse direction by passing smoothly through zero; rather, as illustrated by the graph of $v_\phi^{(1)}$ in Figure 5.3, *the circulation suffers a "1/x-blowup" as the parameters pass through the critical values!* (Of course in deriving the PDE for $v^{(1)}$, it was assumed that $v^{(1)}$ was much smaller than $v^{(0)}$. When this PDE predicts that $v^{(1)}$ is large, the derivation fails. Thus, the blowup of $v^{(1)}$ does not mean that the solution of the full nonlinear problem diverges, but it does mean that the full solution does not depend smoothly on parameters. In other words, the nonlinear solution may be extremely sensitive to perturbations.)

The outline of the paper is as follows. In Section 2, the governing equations are recalled together with Jenike's construction of similarity solutions in conical domains. For nonaxisymmetric domains of the type (1.1), the problem is then linearized about Jenike's solution in Section 3. The resulting system is discretized in Section 4. Numerical results and discussion are offered in Section 5.

2. The model.

2.1. Governing equations and boundary conditions. The unknowns are the 3-component velocity vector v , the 3×3 symmetric stress tensor T , and a scalar plasticity coefficient λ . (The density ρ is a constant.) In total, there are $3+6+1=10$ unknown functions. In writing the equations for these variables, we need the strain rate tensor $V = -1/2(\nabla v + \nabla v^T)$ and the deviatoric part of the stress tensor $\text{dev } T = T - \frac{1}{3} \text{tr } T \mathbf{I}$. Note the sign convention: V measures the *compression* rate of the material; analogously, positive eigenvalues of T correspond to *compressive* stresses.

This sign convention reflects the fact that granular materials disintegrate under tensile stresses.

Following [12], we require that these variables satisfy

$$(2.1) \quad \nabla \cdot T = \rho g,$$

$$(2.2) \quad V = \lambda \operatorname{dev} T,$$

$$(2.3) \quad |\operatorname{dev} T|^2 = 2s^2(\operatorname{tr} T/3)^2,$$

where g is the (vector) acceleration of gravity, $|\cdot|$ denotes the Frobenius norm

$$|T|^2 = \sum_{i,j=1}^3 T_{ij}^2 = \operatorname{tr} T^2$$

(the latter equality only for symmetric tensors) and $s = \sin \delta$, with δ being the angle of internal friction of the material under consideration (see [11]). Equation (2.1) expresses force balance: i.e., Newton's second law with inertia neglected because the flow is assumed slow; it is equivalent to three scalar equations. Equations (2.2) and (2.3) are constitutive laws, the alignment condition and the von Mises yield condition, respectively; they are equivalent to six and to one scalar equations, respectively. Thus (2.1–2.3) is a determined system, 10 equations for 10 unknowns. Since (2.3) contains no derivatives, this system has a differential-algebraic character. Taking the trace of (2.2), we see that $\operatorname{div} v = -\operatorname{tr} V = 0$; thus, incompressibility is part of the constitutive assumptions. Incidentally, for a solution to be physical, the function λ in (2.2) must satisfy $\lambda \geq 0$ everywhere; otherwise friction would be adding energy to the system rather than dissipating it. In fact, we want λ to be strictly positive since one of the assumptions underlying the derivation of (2.1–2.3) is that material is actually deforming.

We seek solutions of (2.1–2.3) in a pyramidal domain, expressed in spherical polar coordinates as

$$(2.4) \quad \Omega = \{(r, \theta, \phi) : 0 \leq \theta < \mathcal{C}(\phi)\},$$

where \mathcal{C} is a given smooth 2π -periodic function. Such a domain represents a mathematical idealization of a converging hopper, in general a nonaxisymmetric one.

On the boundary $\partial\Omega = \{(r, \mathcal{C}(\phi), \phi)\}$, wall impenetrability imposes one boundary condition on the velocity: i.e.,

$$(2.5) \quad v_N = 0,$$

where v_N is the normal velocity. Two additional boundary conditions come from Coulomb's law of sliding friction. The surface traction τ —i.e., the force exerted by the wall on the material—is given by

$$\tau_i = \sum_{j=1}^3 T_{ij} N_j,$$

where N is the unit interior normal to $\partial\Omega$. If the vector τ has normal component τ_N and tangential component $\tau_T = \tau - \tau_N N$, then we require that

$$(2.6) \quad \tau_T = -\mu_w \tau_N (v/|v|),$$

where μ_w is the coefficient of friction between the wall and the material. Note that: (i) If T is positive definite (i.e., if all stresses are compressive), then $\tau_N > 0$. (ii) While τ_N is a scalar, τ_T is effectively a two-component vector; thus, (2.6) is equivalent to two scalar equations. (iii) Because of (2.5), the velocity v is tangential to $\partial\Omega$; we are assuming that $v \neq 0$ at the boundary.

2.2. Jenike's similarity solution. Suppose that the domain (2.4) is axisymmetric: i.e., suppose

$$(2.7) \quad \Omega = \{(r, \theta, \phi) : 0 \leq \theta < \theta_w\},$$

where θ_w is a constant. In this case Jenike [8] found that (2.1–2.3) have solutions that are independent of ϕ and have a similarity dependence on r ,

$$v^{(0)}(r, \theta) = r^{-2} \hat{v}^{(0)}(\theta), \quad T^{(0)}(r, \theta) = r \hat{T}^{(0)}(\theta).$$

(Here and below, a hat above a variable indicates a function that depends on θ alone.) Moreover, only the radial component of velocity is nonzero: i.e., $v_\theta^{(0)} = v_\phi^{(0)} = 0$. Similarly $T_{r\phi}^{(0)} = T_{\theta\phi}^{(0)} = 0$. Indeed all components of T can be expressed in terms of two scalar variables, the so-called Sokolovskii variables [11], the mean stress $p^{(0)} = \text{tr } T^{(0)} / 3$ and an angle ψ ; specifically,

$$(2.8) \quad \text{dev } T^{(0)} = s p^{(0)} \begin{bmatrix} -\frac{2}{\sqrt{3}} \cos 2\psi & -\sin 2\psi & 0 \\ -\sin 2\psi & \frac{1}{\sqrt{3}} \cos 2\psi & 0 \\ 0 & 0 & \frac{1}{\sqrt{3}} \cos 2\psi \end{bmatrix},$$

where $p^{(0)} = r \hat{p}^{(0)}$ and the function ψ , like $\hat{p}^{(0)}$, depends only on θ .

The boundary conditions (2.5, 2.6) may be written more explicitly when Ω is axisymmetric. Equation (2.5) reduces to

$$(2.9) \quad v_\theta = 0.$$

Let us decompose the vector equation (2.6) into a direction and a magnitude. Regarding the direction, the vectors τ_T and v are parallel if

$$(2.10) \quad T_{r\phi} v_\phi - T_{\theta\phi} v_r = 0.$$

Jenike's solution satisfies both (2.9) and (2.10) trivially. The two sides of (2.6) have equal magnitude if

$$(2.11) \quad T_{r\theta} + \mu_w T_{\theta\theta} = 0.$$

We briefly summarize the construction of Jenike's solution, referring to [12] for more details. The ansatz (2.8) arranges that (2.3) holds automatically. On substitution into (2.1), we obtain a first-order 2×2 system of ordinary differential equations for $\hat{p}^{(0)}$ and ψ . This system has a regular singular point at $\theta = 0$, and one boundary condition comes from requiring that the solution be regular there; the other boundary condition comes from (2.11). Thus, the stresses are determined as the solution of a two-point boundary-value problem. (In axial symmetry, the stress equations decouple from the velocity.) Once the stresses are known, (2.2) reduces to a linear first-order ODE for $\hat{v}_r^{(0)}$. The velocity is determined only up to a multiplicative constant, but the normalization of the velocity will scale out of the calculations below.

Incidentally, for Jenike's solution the plasticity coefficient λ in (2.2), which cancels out in the derivation of the equation for $\hat{v}_r^{(0)}$, has the form

$$\lambda^{(0)}(r, \theta) = r^{-4} \hat{\lambda}^{(0)}(\theta).$$

Using (2.2), the function $\hat{\lambda}^{(0)}$ may be determined from $\hat{v}_r^{(0)}$.

3. Linearized analysis for a nearly axisymmetric domain.

3.1. Derivation of linearized differential equations. Equations (2.1–2.3), a 10×10 nonlinear DAE system that is elliptic in the sense of Agmon, Douglis, and Nirenberg [1], present formidable mathematical and numerical challenges. In this paper, we consider a simplified problem that exhibits some astonishing behavior of, and prepares the way for computations with, the full problem on a general domain.

Suppose the function \mathcal{C} specifying the boundary of Ω in (2.4) has the expansion

$$(3.1) \quad \mathcal{C}(\phi) = \theta_w + \epsilon \cos(m\phi) + \mathcal{O}(\epsilon^2)$$

where m is a positive integer. For example, a slightly tilted (circular) cone admits such a representation with $m = 1$, where ϵ measures the angle of tilt; likewise for a (vertical) pyramidal hopper having a slightly elliptical cross section, with $m = 2$.

An expansion of the solution

$$(3.2) \quad v = v^{(0)} + \epsilon v^{(1)} + \mathcal{O}(\epsilon^2), \quad T = T^{(0)} + \epsilon T^{(1)} + \mathcal{O}(\epsilon^2)$$

is sought, where $v^{(0)}, T^{(0)}$ are equal to Jenike's radial solution [8]. Substituting (3.2) into (2.1–2.3), we derive the equations for the first-order perturbation

$$(3.3) \quad \nabla \cdot T^{(1)} = 0,$$

$$(3.4) \quad V^{(1)} = \lambda^{(1)} \text{dev} T^{(0)} + \lambda^{(0)} \text{dev} T^{(1)},$$

$$(3.5) \quad \text{tr}(\text{dev} T^{(0)} \text{dev} T^{(1)}) = 2 s^2 p^{(0)} p^{(1)}$$

where $p^{(i)} = \text{tr} T^{(i)}/3$, $i = 0, 1$ are the mean stresses.

The correction velocity $v^{(1)}$ has the same r -dependence as the Jenike solution [8] (although all three components of $v^{(1)}$ are nonzero), and its ϕ -dependence can be obtained through separation of variables. Indeed, suppose each component of $v^{(1)}$ has the form

$$(3.6) \quad v_j^{(1)} = r^{-2} \hat{v}_j^{(1)}(\theta) \text{trig } m\phi$$

where $\text{trig } m\phi$ denotes either $\cos m\phi$ or $\sin m\phi$. In order to satisfy the appropriately modified version of the boundary condition (2.9) on the perturbed domain, $v_\theta^{(1)}$ will have to be in phase with (3.1): i.e., we need

$$v_\theta^{(1)} = r^{-2} \hat{v}_\theta^{(1)}(\theta) \cos m\phi.$$

It is readily seen that if

$$v_r^{(1)} = r^{-2} \hat{v}_r^{(1)}(\theta) \cos m\phi \quad \text{and} \quad v_\phi^{(1)} = r^{-2} \hat{v}_\phi^{(1)}(\theta) \sin m\phi,$$

then all terms in

$$(3.7) \quad \nabla \cdot v^{(1)} = \partial_r v_r^{(1)} + 2r^{-1} v_r^{(1)} + r^{-1} \partial_\theta v_\theta^{(1)} + r^{-1} \cot \theta v_\theta^{(1)} + r^{-1} \csc \theta \partial_\phi v_\phi^{(1)}$$

$$\begin{array}{ll}
\text{Scalars:} & p = r \hat{p}(\theta) \cos m\phi \\
\text{Vectors:} & v = \frac{1}{r^2} \begin{bmatrix} \hat{v}_r(\theta) \cos m\phi \\ \hat{v}_\theta(\theta) \cos m\phi \\ \hat{v}_\phi(\theta) \sin m\phi \end{bmatrix} \quad \text{Tensors:} \quad T = r \begin{bmatrix} \hat{T}_{rr}(\theta) \cos m\phi \\ \hat{T}_{r\theta}(\theta) \cos m\phi \\ \hat{T}_{\theta\theta}(\theta) \cos m\phi \\ \hat{T}_{r\phi}(\theta) \sin m\phi \\ \hat{T}_{\theta\phi}(\theta) \sin m\phi \\ \hat{T}_{\phi\phi}(\theta) \cos m\phi \end{bmatrix}
\end{array}$$

TABLE 3.1

The r - and ϕ -dependence of scalars, vectors, and tensors in separation of variables

are proportional to $r^{-3} \cos m\phi$: i.e., variables separate in the equation $\nabla \cdot v = 0$.

Tables 3.1–3.3 help systematize the elimination of ϕ -dependence in (3.3–3.5) with separation of variables. The appropriate r - and ϕ -dependence for the scalar $p^{(1)}$, for the vector $v^{(1)}$, and for the tensor $T^{(1)}$ is indicated in Table 3.1. (Note that symmetric 3×3 tensors are represented as vectors in \mathbf{R}^6 , the components being enumerated in the order shown.) In Table 3.2 we record, for the reader's convenience, the expressions in spherical coordinates for four differential operators that occur in these equations.

$$\begin{aligned}
\nabla p &= [\partial_r p, r^{-1} \partial_\theta p, r^{-1} \csc \theta \partial_\phi p]^T \\
\nabla \cdot v &= \partial_r v_r + 2r^{-1} v_r + r^{-1} \partial_\theta v_\theta + r^{-1} \cot \theta v_\theta + r^{-1} \csc \theta \partial_\phi v_\phi \\
V &= \begin{bmatrix} V_{rr} \\ V_{r\theta} \\ V_{\theta\theta} \\ V_{r\phi} \\ V_{\theta\phi} \\ V_{\phi\phi} \end{bmatrix} = - \begin{bmatrix} \partial_r v_r \\ \frac{1}{2} (r^{-1} \partial_\theta v_r - r^{-1} v_\theta + \partial_r v_\theta) \\ r^{-1} (v_r + \partial_\theta v_\theta) \\ \frac{1}{2} (r^{-1} \csc \theta \partial_\phi v_r - r^{-1} v_\phi + \partial_r v_\phi) \\ \frac{1}{2} r^{-1} (\partial_\theta v_\phi - \cot \theta v_\phi + \csc \theta \partial_\phi v_\theta) \\ r^{-1} (v_r + \cot \theta v_\theta + \csc \theta \partial_\phi v_\phi) \end{bmatrix} \\
\nabla \cdot T &= \begin{bmatrix} \partial_r T_{rr} + r^{-1} \csc \theta \partial_\phi T_{r\phi} + r^{-1} \partial_\theta T_{r\theta} + r^{-1} (2T_{rr} - T_{\phi\phi} - T_{\theta\theta} + T_{r\theta} \cot \theta) \\ \partial_r T_{r\theta} + r^{-1} \csc \theta \partial_\phi T_{\theta\phi} + r^{-1} \partial_\theta T_{\theta\theta} + r^{-1} (3T_{r\theta} + (T_{\theta\theta} - T_{\phi\phi}) \cot \theta) \\ \partial_r T_{r\phi} + r^{-1} \csc \theta \partial_\phi T_{\phi\phi} + r^{-1} \partial_\theta T_{\theta\phi} + r^{-1} (3T_{r\phi} + 2T_{\theta\phi} \cot \theta) \end{bmatrix}
\end{aligned}$$

TABLE 3.2

Differential operators in spherical coordinates

The main point, which makes separation of variables work in this problem, is that the θ -dependent part of each of these linear operators is given by

$$\begin{aligned}
(3.8) \quad (a) \quad \widehat{\nabla p} &= (g_1 \partial_\theta + g_0) \hat{p} \\
(b) \quad \widehat{\nabla \cdot v} &= (d_1^T \partial_\theta + d_0^T) \hat{v} \\
(c) \quad \hat{V} &= -(G_1 \partial_\theta + G_0) \hat{v} \\
(d) \quad \widehat{\nabla \cdot T} &= (D_1 \partial_\theta + D_0) \hat{T}
\end{aligned}$$

where g_1, g_0, \dots, D_0 are the matrices given in Table 3.3.

The calculation needed to verify (3.8b) was described above; the other equations may be verified similarly. Incidentally, (3.8a) may be derived by substituting $T = pI$ in (3.8d), and (3.8b) may be derived by taking the trace of (3.8c).

$$\begin{aligned}
g_1 &= \begin{bmatrix} 0 & 1 & 0 \end{bmatrix}^T & g_0 &= \begin{bmatrix} 1 & 0 & \frac{m}{\sin \theta} \end{bmatrix}^T \\
d_1 &= \begin{bmatrix} 0 & 1 & 0 \end{bmatrix}^T & d_0 &= \begin{bmatrix} 0 & \cot \theta & \frac{m}{\sin \theta} \end{bmatrix}^T \\
G_1 &= \begin{bmatrix} 0 & 0 & 0 \\ 1/2 & 0 & 0 \\ 0 & 1 & 0 \\ 0 & 0 & 0 \\ 0 & 0 & 1/2 \\ 0 & 0 & 0 \end{bmatrix} & G_0 &= \begin{bmatrix} -2 & 0 & 0 \\ 0 & -3/2 & 0 \\ 1 & 0 & 0 \\ -\frac{m}{2 \sin \theta} & 0 & -3/2 \\ 0 & -\frac{m}{2 \sin \theta} & -\frac{\cot \theta}{2} \\ 1 & \cot \theta & \frac{m}{\sin \theta} \end{bmatrix} \\
D_1 &= \begin{bmatrix} 0 & 1 & 0 & 0 & 0 & 0 \\ 0 & 0 & 1 & 0 & 0 & 0 \\ 0 & 0 & 0 & 0 & 1 & 0 \end{bmatrix} & D_0 &= \begin{bmatrix} 3 & \cot \theta & -1 & \frac{m}{\sin \theta} & 0 & -1 \\ 0 & 4 & \cot \theta & 0 & \frac{m}{\sin \theta} & -\cot \theta \\ 0 & 0 & 0 & 4 & 2 \cot \theta & -\frac{m}{\sin \theta} \end{bmatrix}
\end{aligned}$$

TABLE 3.3
Matrices in (3.8)

With this notation, (3.3–3.5) reduces to a system of ODEs in θ ,

$$(3.9) \quad (D_1 \partial_\theta + D_0) \hat{T}^{(1)} = 0,$$

$$(3.10) \quad -(G_1 \partial_\theta + G_0) \hat{v}^{(1)} = \hat{\lambda}^{(1)} \text{dev} \hat{T}^{(0)} + \hat{\lambda}^{(0)} \text{dev} \hat{T}^{(1)},$$

$$(3.11) \quad \text{tr}(\text{dev} \hat{T}^{(0)} \text{dev} \hat{T}^{(1)}) = 2 s^2 \hat{p}^{(0)} \hat{p}^{(1)}.$$

Recalling the representation of symmetric tensors as 6-component vectors, we observe that the LHS of (3.11) may be rewritten as an inner product

$$\text{tr}(\text{dev} \hat{T}^{(0)} \text{dev} \hat{T}^{(1)}) = \text{dev} \hat{T}^{(0)T} \mathcal{M} \text{dev} \hat{T}^{(1)}$$

where \mathcal{M} is the 6×6 matrix

$$\mathcal{M} = \text{diag}(1, 2, 1, 2, 2, 1);$$

thus, we may rewrite (3.11) as

$$(3.12) \quad \text{dev} \hat{T}^{(0)T} \mathcal{M} \text{dev} \hat{T}^{(1)} = 2 s^2 \hat{p}^{(0)} \hat{p}^{(1)}.$$

Let us show that the deviatoric stresses in (3.9,3.10,3.12) can be eliminated from these equations to obtain

$$(3.13) \quad (D_1 \partial_\theta + D_0) \left(-\frac{1}{\hat{\lambda}^{(0)}} (G_1 \partial_\theta + G_0) \hat{v}^{(1)} - \frac{\hat{\lambda}^{(1)}}{(\hat{\lambda}^{(0)})^2} \hat{V}^{(0)} \right) + (g_1 \partial_\theta + g_0) \hat{p}^{(1)} = 0$$

$$(3.14) \quad (d_1^T \partial_\theta + d_0^T) \hat{v}^{(1)} = 0$$

where in (3.13)

$$(3.15) \quad \hat{\lambda}^{(1)} = -\frac{1}{2s^2} \frac{1}{(\hat{p}^{(0)})^2 \hat{\lambda}^{(0)}} \hat{V}^{(0)T} \mathcal{M} (G_1 \partial_\theta + G_0) \hat{v}^{(1)} - \frac{\hat{\lambda}^{(0)}}{\hat{p}^{(0)}} \hat{p}^{(1)}.$$

Equation (3.14) follows on taking the trace of (3.10). Next, we rewrite (3.10) as

$$(3.16) \quad \text{dev} \hat{T}^{(1)} = -\frac{1}{\hat{\lambda}^{(0)}}(G_1 \partial_\theta + G_0) \hat{v}^{(1)} - \frac{\hat{\lambda}^{(1)}}{(\hat{\lambda}^{(0)})^2} \hat{V}^{(0)}$$

where we have eliminated $\text{dev} \hat{T}^{(0)}$ using the relation $\hat{V}^{(0)} = \hat{\lambda}^{(0)} \text{dev} \hat{T}^{(0)}$ —effectively, equation (2.2) for Jenike’s solution. Recalling that $\hat{T}^{(1)} = \text{dev} \hat{T}^{(1)} + \hat{p}^{(1)} I$, we substitute (3.16) into (3.9) to derive (3.13). Similarly, (3.15) follows on substituting (3.16) into (3.12) and rearranging.

As a final simplification, we substitute (3.15) into (3.13), obtaining the linear, homogeneous system of ODEs

$$(3.17) \quad -(A_2 \partial_{\theta\theta} + A_1 \partial_\theta + A_0) \hat{v}^{(1)} + (b_1 \partial_\theta + b_0) \hat{p}^{(1)} = 0$$

$$(3.18) \quad (d_1^T \partial_\theta + d_0^T) \hat{v}^{(1)} = 0$$

where, with the definition

$$P = I - \frac{1}{2s^2(\hat{p}^{(0)})^2(\hat{\lambda}^{(0)})^2} \hat{V}^{(0)} \hat{V}^{(0)T} \mathcal{M},$$

the coefficient matrices are given by

$$\begin{aligned} A_2 &= \frac{1}{\hat{\lambda}^{(0)}} D_1 P G_1 \\ A_1 &= \frac{1}{\hat{\lambda}^{(0)}} (D_0 P G_1 + D_1 P G_0) + D_1 \partial_\theta \left(\frac{1}{\hat{\lambda}^{(0)}} P G_1 \right) \\ A_0 &= \frac{1}{\hat{\lambda}^{(0)}} D_0 P G_0 + D_1 \partial_\theta \left(\frac{1}{\hat{\lambda}^{(0)}} P G_0 \right) \\ b_1 &= g_1 + D_1 \frac{\hat{V}^{(0)}}{\hat{p}^{(0)} \hat{\lambda}^{(0)}} \\ b_0 &= g_0 + (D_1 \partial_\theta + D_0) \frac{\hat{V}^{(0)}}{\hat{p}^{(0)} \hat{\lambda}^{(0)}}. \end{aligned}$$

These matrices depend on θ and in fact are singular as $\theta \rightarrow 0$. In Corollary 4.2 below, we show that this system has a six-dimensional solution space.

The combination $1/(\hat{p}^{(0)} \hat{\lambda}^{(0)}) \hat{V}^{(0)}$, which occurs in various places in the above formulas, admits a convenient representation: i.e., combining (2.2) and (2.8) we deduce that

$$(3.19) \quad \frac{1}{\hat{p}^{(0)} \hat{\lambda}^{(0)}} \hat{V}^{(0)} = s \begin{bmatrix} -\frac{2}{\sqrt{3}} \cos 2\psi \\ -\sin 2\psi \\ \frac{1}{\sqrt{3}} \cos 2\psi \\ 0 \\ 0 \\ \frac{1}{\sqrt{3}} \cos 2\psi \end{bmatrix}$$

The following supplementary information will be needed in Section 4.

LEMMA 3.1. *Under the reflection $\theta \mapsto -\theta$, the functions in separation of variables have the parities*

$$(3.20) \quad \begin{aligned} (a) \quad & \hat{p}(-\theta) = (-1)^m \hat{p}(\theta), & (b) \quad \hat{v}_r^{(1)}(-\theta) &= (-1)^m \hat{v}_r^{(1)}(\theta) \\ (c) \quad & \hat{v}_\theta^{(1)}(-\theta) = (-1)^{m+1} \hat{v}_\theta^{(1)}(\theta), & (d) \quad \hat{v}_\phi^{(1)}(-\theta) &= (-1)^{m+1} \hat{v}_\phi^{(1)}(\theta). \end{aligned}$$

$$\begin{aligned}
A_2(\theta) &= \begin{bmatrix} \frac{1}{2} & 0 & 0 \\ 0 & \frac{5}{6} & 0 \\ 0 & 0 & \frac{1}{2} \end{bmatrix} + \mathcal{O}(\theta) \\
A_1(\theta) &= \theta^{-1} \begin{bmatrix} \frac{1}{2} & 0 & 0 \\ 0 & \frac{5}{6} & \frac{m}{3} \\ 0 & -\frac{m}{3} & \frac{1}{2} \end{bmatrix} + \mathcal{O}(1) \\
A_0(\theta) &= \theta^{-2} \begin{bmatrix} -\frac{m^2}{2} & 0 & 0 \\ 0 & -\frac{m^2}{2} - \frac{5}{6} & -\frac{4m}{3} \\ 0 & -\frac{4m}{3} & -\frac{5m^2}{6} - \frac{1}{2} \end{bmatrix} + \mathcal{O}(\theta^{-1}) \\
b_1(\theta) &= (1 + s/\sqrt{3}) \begin{bmatrix} 0 & 1 & 0 \end{bmatrix}^T + \mathcal{O}(\theta) \\
b_0(\theta) &= \theta^{-1}(1 + s/\sqrt{3}) \begin{bmatrix} 0 & 0 & -m \end{bmatrix}^T + \mathcal{O}(1) \\
d_1(\theta) &= \begin{bmatrix} 0 & 1 & 0 \end{bmatrix}^T \quad (\text{exactly}) \\
d_0(\theta) &= \theta^{-1} \begin{bmatrix} 0 & 1 & m \end{bmatrix}^T + \mathcal{O}(1)
\end{aligned}$$

TABLE 3.4

Leading-orders in the expansions at $\theta = 0$ of the coefficient matrices of (3.17–3.18)

Proof. The reflection $\theta \mapsto -\theta$ and the rotation $\phi \mapsto \phi + \pi$ are different representations of the same mapping. Therefore, since p is a scalar

$$\hat{p}(-\theta) \cos m\phi = \hat{p}(\theta) \cos m(\phi + \pi) = (-1)^m \hat{p}(\theta) \cos m\phi,$$

which proves (3.20a). Equation (3.20b) follows from the same argument since v_r transforms as a scalar under changes in the angular coordinates. Rather than analyze the parities of v_θ and v_ϕ , we prefer an indirect argument. Since $\nabla \cdot v^{(1)}$ is a scalar, $\nabla \cdot v^{(1)}$ has parity $(-1)^m$ under the reflection $\theta \mapsto -\theta$, and on inspecting (3.7), we deduce (3.20c,d). \square

Incidentally, although we shall not need that information below, we remark that under this reflection \hat{T}_{rr} , $\hat{T}_{\theta\theta}$, $\hat{T}_{\phi\phi}$, and $\hat{T}_{\phi\phi}$ have parity $(-1)^m$ while $\hat{T}_{r\theta}$ and $\hat{T}_{\phi r}$ have parity $(-1)^{m+1}$.

3.2. Boundary conditions at the centerline. Equations (3.17,3.18) have a regular singular point at $\theta = 0$. The leading orders of the coefficient matrices in these equations are given in Table 3.4. This information may be determined *without knowing the Jenike solution explicitly* since, using the fact that $\psi(0) = 0$, we deduce from (3.19) that

$$\frac{\hat{V}^{(0)}}{\hat{p}^{(0)}\hat{\lambda}^{(0)}}(0) = \frac{s}{\sqrt{3}} \begin{bmatrix} -2 & 0 & 1 & 0 & 0 & 1 \end{bmatrix}^T.$$

According to the method of Frobenius [3], equations (3.17,3.18) admit solutions of the form

$$(3.21) \quad \hat{v}^{(1)}(\theta) = \theta^\nu F(\theta), \quad \hat{p}^{(1)}(\theta) = \theta^{\nu-1} f(\theta)$$

where $F(\theta)$ and $f(\theta)$ are analytic near $\theta = 0$. Suppose the exponent ν is real; if $1 \leq \nu$ such a solution is continuous, if $\nu < 0$ it is singular, and if $0 \leq \nu < 1$ it is continuous provided $f(0) = 0$.

PROPOSITION 3.2. *There are exactly three linearly independent solutions of (3.17,3.18) of the form (3.21) that are continuous at $\theta = 0$.*

Proof. Substitution of (3.21) into (3.17,3.18) gives an indicial equation with roots

$$(3.22) \quad \nu = \pm(m+1), \pm m, \pm(m-1).$$

First suppose $m \geq 2$. Since three of the roots (3.22) are negative, there are *at most* three continuous solutions. However, because the positive roots differ by integers, these roots might produce fewer than three continuous solutions: the solutions corresponding to the exponents $\nu = m$ or $\nu = m-1$ might contain log terms. Nevertheless, using Maple we have verified that this possibility does not arise—all three values of ν produce continuous solutions.

If $m = 1$, there are four nonnegative roots (3.22), with zero being a double root. Again using Maple we have eliminated the various alternative possibilities to show that there are, in fact, exactly three linearly independent continuous solutions. See Section 5.3 for more details about the Maple code. \square

Incidentally, since the roots of the indicial equation are integers, the continuous solutions of the lemma are actually *analytic* near $\theta = 0$.

As noted above, we prove in Corollary 4.2 that equations (3.17,3.18) have a six-dimensional solution space. (This fact also emerges in the Maple computation.) Thus, the condition that solutions be regular at $\theta = 0$ is equivalent to three boundary conditions. Therefore, regularity at $\theta = 0$ plus the three boundary conditions (2.5,2.6) will provide a complete set of boundary conditions.

3.3. Boundary conditions at the hopper wall. We derive the perturbed version of (2.5) in some detail; similar issues arise for (2.6), and we treat the latter equation more succinctly. The calculations are greatly simplified by the fact that we may neglect any quantity that is $\mathcal{O}(\epsilon^2)$. To exploit this simplification efficiently, we temporarily use the notation $F \sim G$ to mean that $F = G + \mathcal{O}(\epsilon^2)$.

Including a prefactor of r^2 to remove all r -dependence from the equation, we may rewrite (2.5) as

$$(3.23) \quad r^2 v(r, \theta_w + \epsilon \cos m\phi, \phi) \cdot N = 0.$$

Because of the perturbation, (3.23) differs from (2.9) in three respects:

- the velocity v contains an additional term, $v \sim v^{(0)} + \epsilon v^{(1)}$;
- the velocity is evaluated at a location shifted by $\epsilon \cos m\phi$, and
- the direction of the normal N is changed.

Regarding the first two points, we observe that

$$r^2 v(r, \theta_w + \epsilon \cos m\phi, \phi) \sim \hat{v}^{(0)}(\theta_w) + \epsilon \cos m\phi \partial_\theta \hat{v}^{(0)}(\theta_w) + \epsilon \text{trig } m\phi \hat{v}^{(1)}(\theta_w)$$

where $\text{trig } m\phi$ equals $\cos m\phi$ or $\sin m\phi$, depending on the component of $\hat{v}^{(1)}$. Regarding the third point, $\partial\Omega$ is the zero set of the function $\theta - \theta_w - \epsilon \cos m\phi$. Taking the gradient of this function, we conclude that the (inward) normal is

$$N \sim \begin{bmatrix} 0 & -1 & -\epsilon \frac{\sin m\phi}{\sin \theta_w} \end{bmatrix}^T.$$

Modulo an $\mathcal{O}(\epsilon^2)$ -error, N has unit length. Substituting the previous two equations into (3.23), we deduce that

$$\begin{aligned} -r^2 v(r, \theta_w + \epsilon \cos m\phi, \phi) \cdot N &\sim \hat{v}_\theta^{(0)}(\theta_w) + \epsilon \cos m\phi \left(\partial_\theta \hat{v}_\theta^{(0)}(\theta_w) + \hat{v}_\theta^{(1)}(\theta_w) \right) \\ &\quad + \epsilon \frac{\sin m\phi}{\sin \theta_w} \hat{v}_\phi^{(0)}(\theta_w). \end{aligned}$$

However, since $v_\theta^{(0)}$ and $v_\phi^{(0)}$ vanish identically for Jenike's solution, the velocity boundary condition for the perturbed problem reduces to

$$(3.24) \quad \hat{v}_\theta^{(1)}(\theta_w) = 0.$$

We turn to the stress boundary condition (2.6). As regards the scalar τ_N in (2.6), we observe that, since $T_{r\phi}^{(0)}$ and $T_{\theta\phi}^{(0)}$ vanish for Jenike's solution,

$$(3.25) \quad \tau_N = \sum_{i,j=1}^3 T_{ij} N_i N_j \sim T_{\theta\theta}^{(0)} + \epsilon T_{\theta\theta}^{(1)}.$$

The vectors τ_T and v_T in (2.6) lie in a two-dimensional subspace tangent to $\partial\Omega$. Note that the unperturbed tangent space is spanned by the r and ϕ coordinate directions. Even allowing for the perturbation, the two sides of (2.6) will be equal iff their r - and ϕ -components are equal; in symbols, iff

$$\begin{bmatrix} \tau_{Tr} \\ \tau_{T\phi} \end{bmatrix} = -\frac{\mu_w \tau_N}{|v|} \begin{bmatrix} v_r \\ v_\phi \end{bmatrix}.$$

This equality will hold iff (i) the two sides of the equation are parallel vectors and (ii) the first components of the two sides are equal; again, in symbols, iff

$$(3.26) \quad \tau_{Tr} v_\phi - \tau_{T\phi} v_r = 0 \quad \text{and}$$

$$(3.27) \quad \tau_{Tr} + \mu_w \tau_N (v_r / |v|) = 0.$$

Regarding v , it is clear that

$$(3.28) \quad \begin{bmatrix} v_r \\ v_\phi \end{bmatrix} \sim \begin{bmatrix} v_r^{(0)} \\ 0 \end{bmatrix} + \epsilon \begin{bmatrix} v_r^{(1)} \\ v_\phi^{(1)} \end{bmatrix}.$$

Regarding $\tau_T = \tau - \tau_N N$, we claim that

$$(3.29) \quad \begin{bmatrix} \tau_{Tr} \\ \tau_{T\phi} \end{bmatrix} \sim - \begin{bmatrix} T_{r\theta}^{(0)} \\ 0 \end{bmatrix} - \epsilon \begin{bmatrix} T_{r\theta}^{(1)} \\ T_{\theta\phi}^{(1)} \end{bmatrix}.$$

Verifying this claim is straightforward except that, in analyzing the second component, one must invoke the fact that Jenike's solution satisfies $T_{\theta\theta}^{(0)} = T_{\phi\phi}^{(0)}$. On substituting (3.28) and (3.29) into (3.26), we obtain the equation

$$\epsilon \left(T_{r\theta}^{(0)} v_\phi^{(1)} - v_r^{(0)} T_{\theta\phi}^{(1)} \right) = 0 \quad \text{at } \theta = \theta_w + \epsilon \cos m\phi.$$

The difference between evaluating this expression at $\theta = \theta_w$ and at the perturbed location is $\mathcal{O}(\epsilon^2)$. Removing the r -dependence (proportional to r) and the ϕ -dependence

(proportional to $\sin m\phi$) from this equation, we obtain the first stress boundary condition for the perturbed problem:

$$(3.30) \quad \left(\hat{T}_{r\theta}^{(0)} \hat{v}_\phi^{(1)} - \hat{v}_r^{(0)} \hat{T}_{\theta\phi}^{(1)} \right) = 0 \quad \text{at } \theta = \theta_w.$$

Regarding (3.27), we claim that

$$|v| = \sqrt{v_r^2 + v_\theta^2 + v_\phi^2} \sim |v_r|.$$

Indeed, it is clear from (3.28) that the contribution of v_ϕ to $|v|$ is $\mathcal{O}(\epsilon^2)$, and by (3.24) the contribution of v_θ to $|v|$ is $\mathcal{O}(\epsilon^4)$. Thus, $v_r/|v| \sim -1$. Substituting (3.25) and (3.29) into (3.27), we obtain the condition

$$(T_{r\theta}^{(0)} + \epsilon T_{r\theta}^{(1)}) + \mu_w (T_{\theta\theta}^{(0)} + \epsilon T_{\theta\theta}^{(1)}) \sim 0 \quad \text{at } \theta = \theta_w + \epsilon \cos m\phi.$$

By (2.11), $T_{r\theta}^{(0)} + \mu_w T_{\theta\theta}^{(0)}$ vanishes at $\theta = \theta_w$, but at the perturbed location these terms make an $\mathcal{O}(\epsilon)$ -contribution. Allowing for this contribution and eliminating the r - and ϕ -dependence, we derive the second stress boundary condition for the perturbed problem:

$$(3.31) \quad \hat{T}_{r\theta}^{(1)} + \mu_w \hat{T}_{\theta\theta}^{(1)} = -\partial_\theta \left(\hat{T}_{r\theta}^{(0)} + \mu_w \hat{T}_{\theta\theta}^{(0)} \right) \quad \text{at } \theta = \theta_w.$$

We have put the inhomogeneous term, which does not involve the perturbation $T^{(1)}$, on the right side of the equation. (By contrast, (3.30) and (3.24) are homogeneous.)

It is noteworthy that the perturbed boundary conditions (3.30, 3.31) resemble (2.10, 2.11) rather closely.

4. Numerical approximation of the 2-point BVP. The coefficients in (3.17, 3.18) depend on the zeroth-order solution discussed in Section 2.2. This solution can be found numerically without difficulty, see e.g. [7] where a shooting method is used or [11]. We will consider the zeroth-order solution as given, and we will focus on the corrections $\hat{v}^{(1)}$ and $\hat{p}^{(1)}$.

To simplify the notation before discretization, we set

$$w = \hat{v}^{(1)}, \quad z = \frac{d}{d\theta} \hat{v}^{(1)} \quad \text{and} \quad q = \hat{p}^{(1)}$$

and rewrite equations (3.17, 3.18) as a first-order system

$$(4.1) \quad \begin{bmatrix} \mathbf{I} & 0 & 0 \\ 0 & -A_2 & b_1 \\ 0 & 0 & 0 \end{bmatrix} \begin{bmatrix} w' \\ z' \\ q' \end{bmatrix} + \begin{bmatrix} 0 & -\mathbf{I} & 0 \\ -A_0 & -A_1 & b_0 \\ d_0^T & d_1^T & 0 \end{bmatrix} \begin{bmatrix} w \\ z \\ q \end{bmatrix} = \begin{bmatrix} 0 \\ 0 \\ 0 \end{bmatrix},$$

where the coefficient matrices are the same as above. The system (4.1) is completed by the three boundary conditions (3.24, 3.30, 3.31).

The above system (4.1) is differential-algebraic; in the next lemma we show it has index one. (The meaning of this term is defined in the proof, or see [4].) The approximation of solutions of the initial-value problem for such low-index DAEs is relatively well-understood; see for instance [4] for convergence results. Moreover, some results for the initial-value problem may be extended to boundary-value problems, see [5]. These considerations provide a theoretical justification for our using the midpoint rule to solve (4.1) numerically.

LEMMA 4.1. *Assuming downward flow, i.e., $v_r(\theta) < 0$ for any θ , the first-order system is differential-algebraic of index one.*

Proof. We need to show that by differentiating some of the components of (4.1) at most once, the algebraic character of the system can be eliminated, leaving a purely differential equation. Let us differentiate only the last component of (4.1),

$$(4.2) \quad d_0^T w + d_1^T z = 0.$$

The resulting system may be written

$$(4.3) \quad \begin{bmatrix} I & 0 & 0 \\ 0 & -A_2 & b_1 \\ 0 & d_1^T & 0 \end{bmatrix} \begin{bmatrix} w' \\ z' \\ q' \end{bmatrix} + \begin{bmatrix} \text{linear} \\ \text{zeroth-order} \\ \text{terms} \end{bmatrix} = 0.$$

We claim the coefficient matrix in (4.3) is nonsingular. Then, multiplying (4.3) by the inverse of this matrix, we obtain a purely differential equation.

To prove the claim, it suffices to show that

$$(4.4) \quad B = \begin{bmatrix} +\hat{\lambda}^{(0)} A_2 & b_1 \\ d_1^T & 0 \end{bmatrix}$$

is nonsingular, where, without changing invertibility we have inserted a factor of $-\hat{\lambda}^{(0)}$ in the upper left, which simplifies the calculation. Let us introduce the notation W for the column vector on the RHS of (3.19), so that $1/(\hat{p}^{(0)} \hat{\lambda}^{(0)}) \hat{V}^{(0)} = sW$. Then from the definitions following (3.17, 3.18), we have $b_1 = g_1 + D_1 W$. Similarly, regarding A_2 , since $\mathcal{M}G_1 = D_1^T$, we have $\hat{\lambda}^{(0)} A_2 = D_1 G_1 - \frac{1}{2}(D_1 W)(D_1 W)^T$. But

$$D_1 W = \begin{bmatrix} -\sin 2\psi & \frac{1}{\sqrt{3}} \cos 2\psi & 0 \end{bmatrix}^T.$$

Hence the matrix (4.4) equals

$$B = \begin{bmatrix} \frac{1}{2} - \frac{1}{2} \sin^2 2\psi & * & * & -s \sin 2\psi \\ \frac{1}{2\sqrt{3}} \cos 2\psi \sin 2\psi & * & * & 1 + \frac{s}{\sqrt{3}} \cos 2\psi \\ 0 & 0 & \frac{1}{2} & 0 \\ 0 & 1 & 0 & 0 \end{bmatrix}$$

where $*$ indicates elements that do not affect the invertibility of B . It is readily calculated that

$$\det B = -\frac{1}{4} \left(\cos^2 2\psi + \frac{s}{\sqrt{3}} \cos 2\psi \right).$$

As shown on p.43 of [12], the assumption that $v_r^{(0)} < 0$ implies that $|\psi(\theta)| < \pi/4$, and the claim follows. \square

COROLLARY 4.2. *The solution space of (4.1) has dimension six.*

Proof. The solution space of (4.3), which is seven dimensional, may be parameterized by initial values $\begin{bmatrix} w(\theta_0) & z(\theta_0) & q(\theta_0) \end{bmatrix}^T$. Since (4.3) was obtained from (4.1) by differentiating (4.2), we conclude that for a solution of (4.3),

$$d_0^T w(\theta) + d_1^T z(\theta) \equiv 0 \quad \text{if and only if} \quad d_0^T w(\theta_0) + d_1^T z(\theta_0) = 0.$$

Thus the solution space of (4.1) may be identified with the set of solutions of (4.3) whose initial conditions satisfy the scalar equation (4.2). \square

The boundary value problem (4.1), (3.24, 3.30, 3.31) is discretized using a symmetric implicit Runge-Kutta method [2], [4]. Since the solutions are expected to behave smoothly with respect to θ , the simplest of those methods, namely the midpoint rule, is chosen. In spite of being only second order accurate, this choice is shown to be adequate below. The interval $(0, \theta_w)$ is divided in N subintervals of size $\Delta\theta = \theta_w/N$, defining a uniform mesh with nodes $\theta_i = i \Delta\theta$, $i = 0, 1, \dots, N$. At each grid point θ_i there are seven unknowns,

$$U^i = [w_1^i \ w_2^i \ w_3^i \ z_1^i \ z_2^i \ z_3^i \ q^i]^T.$$

Since there are $N + 1$ grid points, there are $7(N + 1)$ unknowns in total. The midpoint rule for the ODE (4.1) is applied on each interval $[\theta_{i-1}, \theta_i]$, $i = 1, \dots, N$, leading to $7N$ equations for the $7(N + 1)$ unknowns.

Seven additional equations are needed to close the system, and these are provided by the boundary conditions. At $\theta = \theta_w$, the three conditions (3.24, 3.30, 3.31) are imposed; and at $\theta = 0$, the four numerical boundary conditions listed in Table 4.1 are imposed. The latter boundary conditions may be justified as follows. According to (3.21, 3.22), as $\theta \rightarrow 0$,

$$w \sim \theta^\nu, \quad q \sim \theta^{\nu-1},$$

where $\nu \geq m - 1$. Thus $w(0) = 0$ if $m \geq 2$, and $q(0) = 0$ if $m \geq 3$. In fact, if $m = 2$, direct calculation of the Frobenius solution (3.21) shows that $q(0) = 0$ remains true in this case too. If $m = 1$, we refer to Lemma 3.1: by parity, w_1 , q , and $z_3 = dw_3/d\theta$ all vanish at $\theta = 0$. The fourth boundary condition in Table 4.1 follows from the last equation in (4.1) in the limit $\theta \rightarrow 0$.

$m = 1$	$w_1^0 = 0$	$w_2^0 + w_3^0 = 0$	$z_3^0 = 0$	$q^0 = 0$
$m \geq 2$	$w_1^0 = 0$	$w_2^0 = 0$	$w_3^0 = 0$	$q^0 = 0$

TABLE 4.1
Numerical boundary conditions at $\theta = 0$.

The resulting $7(N + 1) \times 7(N + 1)$ system has the following structure

$$(4.5) \quad \begin{bmatrix} S_1 & R_1 & & & & \\ & S_2 & R_2 & & & \\ & & & \ddots & & \\ & & & & S_N & R_N \\ B_0 & & & & & B_w \end{bmatrix} \begin{bmatrix} U^0 \\ U^1 \\ \vdots \\ U^{N-1} \\ U^N \end{bmatrix} = \begin{bmatrix} 0 \\ 0 \\ \vdots \\ 0 \\ Q \end{bmatrix}$$

The last row of the above system corresponds to the implementation of the boundary conditions; the 7×7 matrices B_0 and B_w contain the coefficients entering in the formula from Table 4.1 and (3.24, 3.30, 3.31) respectively, while Q corresponds to the nonhomogeneous part of the boundary condition (3.31).

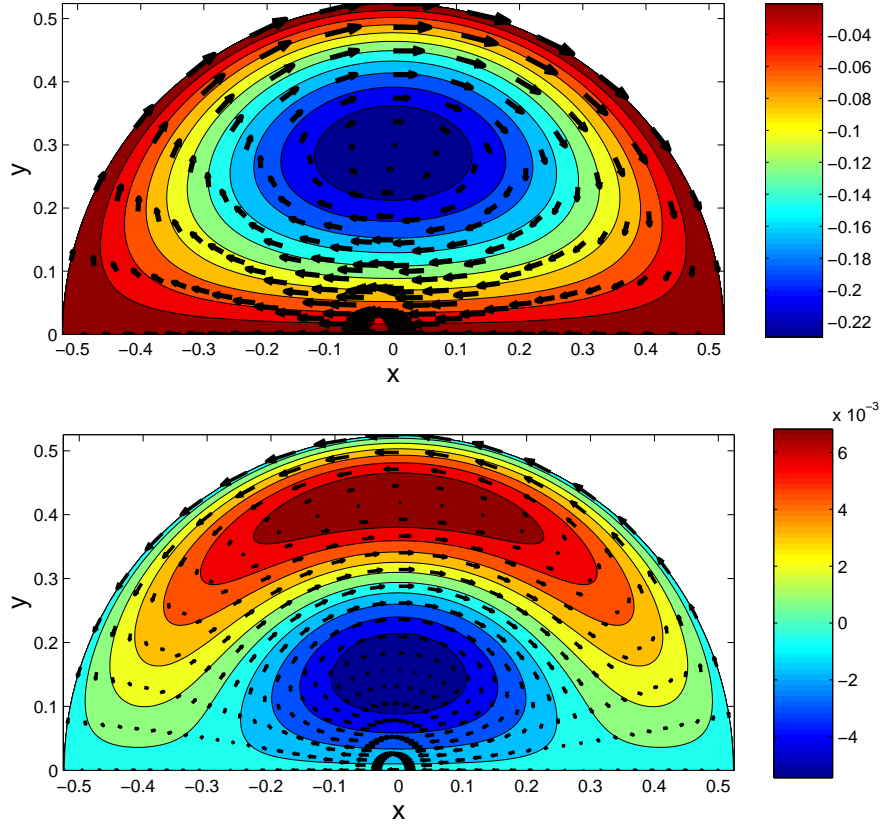


FIG. 5.1. Stream function showing secondary flow in a tilted hopper ($m = 1$, $\theta_w = 30^\circ$, $\delta = 30^\circ$); top: angle of wall friction = 15° ($\mu_w = \tan 15^\circ$), bottom: angle of wall friction = 23.3° ($\mu_w = \tan 23.3^\circ$). By symmetry, only half of the hopper is represented.

5. Numerical results.

5.1. Secondary circulation. We claim that, for solutions of (4.1), secondary circulation—i.e., flow tangential to the spherical cap $\{r = \text{const}\}$ —may be described in terms of the stream function

$$\Psi = \frac{1}{mr} \sin \theta \sin m\phi w_2(\theta).$$

In other words, we must show that

$$(5.1) \quad (a) v_\theta^{(1)} = \frac{1}{r \sin \theta} \partial_\phi \Psi, \quad (b) v_\phi^{(1)} = -\frac{1}{r} \partial_\theta \Psi.$$

Since $v_\theta^{(1)} = r^{-2} w_2(\theta) \cos m\phi$, equation (5.1a) follows by direct differentiation. On the other hand, since $v_r^{(1)} = r^{-2} w_1(\theta) \cos m\phi$, we have $(\partial_r + 2r^{-1})v_r = 0$, so by (3.7)

$$(\partial_\theta + \cot \theta) w_2(\theta) \cos m\phi + \csc \theta w_3(\theta) \partial_\phi (\sin m\phi) = 0,$$

from which (5.1b) follows.

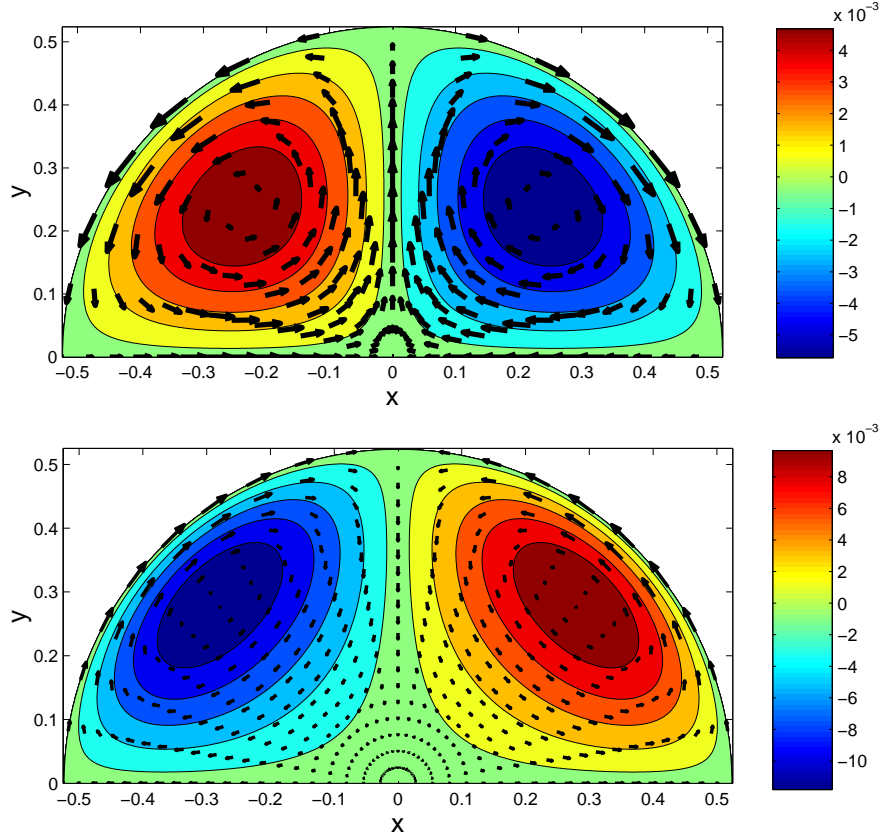


FIG. 5.2. Stream function showing secondary flow in an “elliptical” ($m = 2$, $\theta_w = 30^\circ$, $\delta = 30^\circ$); top: angle of wall friction = 15° ($\mu_w = \tan 15^\circ$), bottom: angle of wall friction = 23.3° ($\mu_w = \tan 23.3^\circ$).

Figures 5.1 and 5.2 show plots of the level lines of Ψ , which equal the projection of the streamlines onto a spherical cap $\{r = \text{const}\}$. Figure 5.1 corresponds to a tilted hopper ($m = 1$), while Figure 5.2 corresponds to an “elliptical” hopper ($m = 2$). In both cases, two different values of the wall friction are presented, while the other parameters are held constant. The grains do not move along radial lines but follow more complicated and fully three-dimensional trajectories. One can observe from Figures 5.1 and 5.2 that the sign of the main circulation changes when μ_w increases. In the case $m = 1$, this is even accompanied by a change in the topology of the flow—i.e., the addition of a vortex.

As μ_w varies between the values shown in the Figures, the flows do *not* undergo a smooth transition from one case to the other. This is demonstrated in Figure 5.3 which shows, for values of m from 1 to 4, the azimuthal velocity $\hat{v}_\phi^{(1)}(\theta_w)$ on the wall as a function of the wall friction μ_w . For each value of m , $\hat{v}_\phi^{(1)}$ suffers a “ $1/x$ -blowup” as μ_w passes through a critical value.

As μ_w crosses the critical values in Figure 5.3, the direction of the circulation changes in a singular way. It turns out that there are also additional critical parameter values for which the sign of the circulation changes *smoothly*, passing continuously

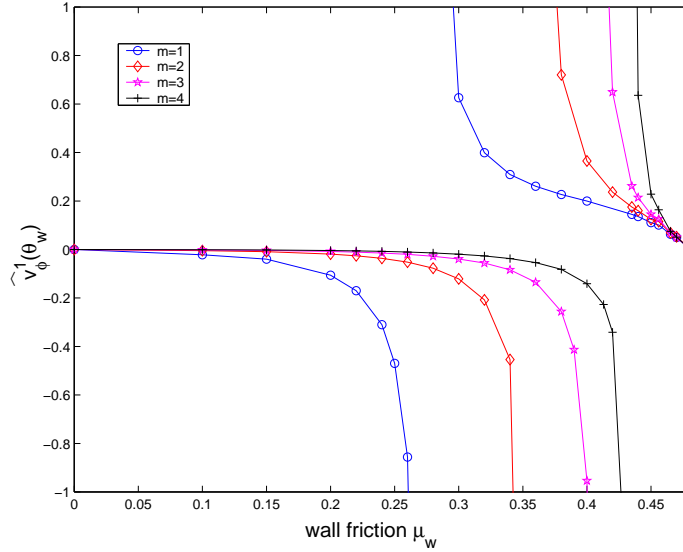


FIG. 5.3. Dependence of the resonance on the geometry of the domain through the coefficient m : blowup of $\hat{v}_\phi^{(1)}(\theta_w)$ as a function of the wall friction μ_w (internal friction $\delta = 30^\circ$, half opening angle $\theta_w = 30^\circ$).

through zero. For the case $m = 1$ and $\delta = 30^\circ$, curves of θ_w , μ_w along which the circulation changes sign by either mechanism are shown in Figure 5.4. Note that the smooth-transition curve does not depend on the value of m , but is a property of the radial solution itself. Specifically, the circulation vanishes when the boundary condition for the correction terms (3.31) is homogeneous, i.e., $\partial_\theta \hat{T}_{r\theta}^{(0)} + \mu_w \partial_\theta \hat{T}_{\theta\theta}^{(0)} = 0$ at $\theta = \theta_w$. The range of θ_w in Figure 5.4 is limited by the mass-flow limit—exceeding this limit leads to flows with rigid regions, to which the present model does not apply. The range of μ_w is limited by the condition that $\mu_w < \sin \delta = 1/2$; here the upper bound corresponds to a fully rough wall [8].

Figure 5.5 offers a three-dimensional view of which combinations of the parameters δ , μ_w and θ_w lead to blowup. Another surface of critical values corresponds to the above mentioned smooth transitions. In Figure 5.5, the curve of intersection between those two critical surfaces is also represented.

5.2. Relation to bifurcation theory. While the blowup in the correction solution could not have been anticipated, its cause is easily understood *a posteriori*. The two-point boundary problem for $\hat{v}^{(1)}$, $\hat{T}^{(1)}$ has inhomogeneous boundary conditions, but at the singular point, the problem with the corresponding homogeneous boundary condition

$$(5.2) \quad \hat{T}_{r\theta}^{(1)} + \mu_w \hat{T}_{\theta\theta}^{(1)} = 0 \quad \text{at } \theta = \theta_w$$

has a nonzero solution. This behavior is analogous to that of a forced harmonic oscillator

$$\ddot{x} + \omega_0^2 x = A \sin \omega t.$$

The steady state oscillations have amplitude $A/(\omega_0^2 - \omega^2)$ which diverges as ω passes through the natural frequency ω_0 of the oscillator. Unlike the above problem, in our

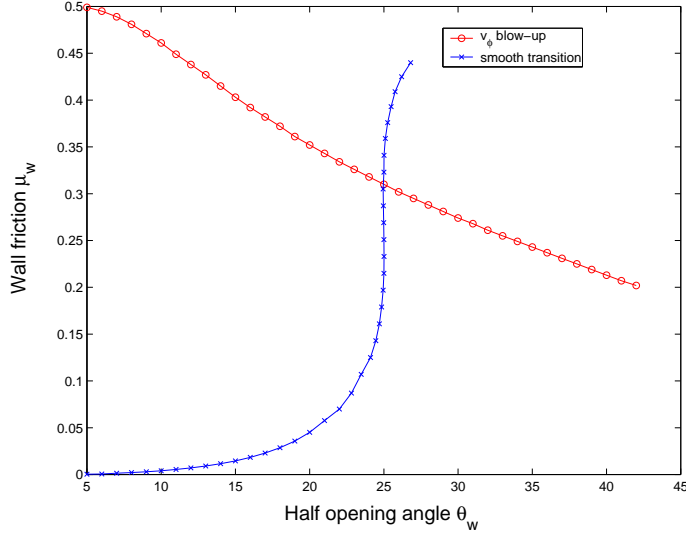


FIG. 5.4. Critical values leading to sign changes of the circulation (internal friction $\delta = 30^\circ$, $m = 1$).

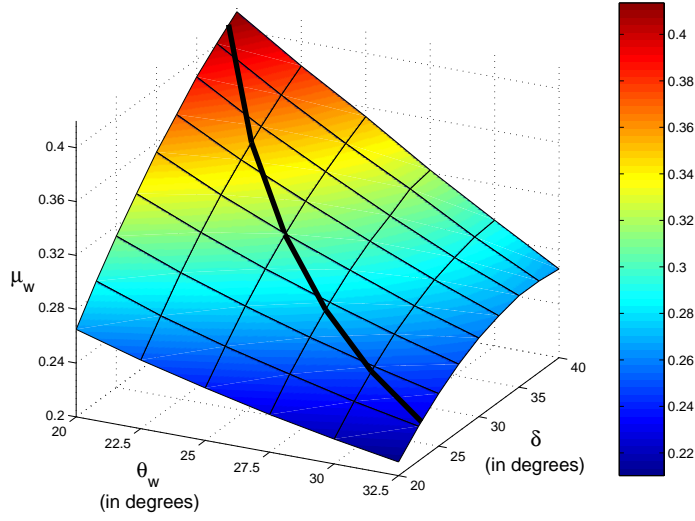


FIG. 5.5. Locus of parameters for which blowup of $\hat{v}^{(1)}$ occurs ($m = 1$.) The dark curve represents the intersection of this surface with the locus of parameters for which the flow changes direction smoothly. Compare with 5.4.

model the inhomogeneity is in a boundary condition rather than the equation.

These remarks suggest a connection with bifurcation theory. Consider equations (2.1–2.3) on the conical domain $\{0 \leq \theta < \theta_w\}$ subject to boundary conditions (2.9–2.11). Let us write $W = [v, T, \lambda]^T$ as a multicomponent unknown, and from the three parameters δ, μ_w, θ_w let us consider μ_w as a distinguished (bifurcation) parameter. We rewrite (2.1–2.3), (2.9–2.11) symbolically as

$$(5.3) \quad \Phi(W, \mu_w) = 0.$$

Now for any μ_w , the Jenike solution $W^{(0)}$ provides one solution of (5.3). We investigate other possible solutions of this equation with the implicit function theorem. Let L be the linearization of Φ with respect to its first argument: i.e.,

$$L\bar{W} = \lim_{h \rightarrow 0} h^{-1} \left(\Phi(W^{(0)} + h\bar{W}, \mu_w) - \Phi(W^{(0)}, \mu_w) \right).$$

If L is invertible, then the Jenike solution is the unique solution of (5.3) in some neighborhood of $W^{(0)}$. Thus, to detect possible bifurcation, we look for values of μ_w such that there is a nonzero solution of the equation

$$(5.4) \quad L\bar{W} = 0.$$

Essentially, we have already calculated L . In linearizing the PDEs (2.1–2.3) we obtain (3.3–3.5). In linearizing boundary conditions, (2.9) becomes (3.24); (2.10) becomes (3.30); and, because the location of the boundary is not moved, (2.11) becomes not (3.31) but (5.2). By the above analysis, (5.4) has a nonzero solution precisely when μ_w equals a critical value at which the correction solution blows up.

In light of bifurcation theory [6], these observations lead us to make the following conjecture: *Even in a conical domain, there are solutions of (5.3) with nonzero circulation. These bifurcate from the Jenike solution where μ_w equals a critical value.* We shall explore this conjecture in a future publication.

5.3. Checks on the computation. For comparison with the above numerical solution, the method of Frobenius was applied directly to the system (3.17,3.18) using Maple. Given Jenike's radial field, a linear system for the coefficients of the series solution is readily formed and solved, yielding a solution with three free parameters, corresponding to the three linearly independent solutions in Proposition 3.2. Subsequently, the three boundary conditions (3.24,3.30,3.31) provide the needed relations to determine the solution to the full boundary value problem.

Two methods of obtaining the radial field were employed. Under the assumption that θ_w^2 and μ_w/θ_w are both small and of the same order, a series representation of the Jenike field was computed within Maple itself. Under the less restrictive assumption that only θ_w be small (say 10°), numerical solutions were computed in MATLAB, fitted to polynomials, and then imported into Maple. In both cases, the resulting polynomials were then used to compute the first order correction. The corrections

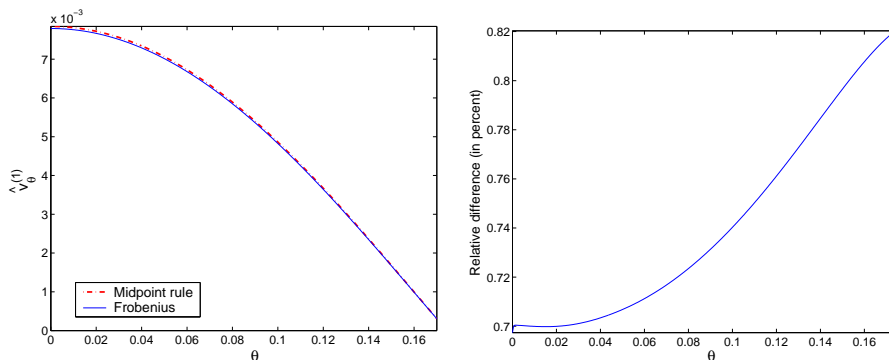


FIG. 5.6. Comparison of $v_\theta^{(1)}$ from the purely numerical method of Section 4 and from the Frobenius method of Section 5.3. (Using $m = 1$, $\theta_w = 10^\circ$, $\delta = 30^\circ$, and $\mu_w = 0.3$.)

to the stress and velocity obtained through this symbolic approach agree extremely well with the results of the purely numerical method of Sections 4 and 5: for the representative values $\theta_w = 10^\circ$, $\delta = 30^\circ$, and $\mu_w = 0.3$ the corrections obtained by the two different methods have a relative difference of less than 1%. Furthermore, with $\theta_w = 10^\circ$ and $\delta = 30^\circ$ the corrections obtained via Maple exhibited the familiar “ $1/x$ -blowup” near $\mu_w = 0.4605$. For comparison, in the purely numerical approach, at the same values of δ and θ_w , blowup occurred for $\mu_w = 0.4610$.

Acknowledgments. The authors thank Bob Behringer, Steve Campbell, Tim Kelley, Tony Royal and Michael Shearer for many helpful discussions.

REFERENCES

- [1] S. AGMON, A. DOUGLIS, AND L. NIRENBERG,, *Estimates near the boundary for solutions of elliptic partial differential equations satisfying general boundary conditions II*, Comm. Pure Appl. Math., 17 (1964), pp. 35–92.
- [2] U.M. ASCHER AND L.R. PETZOLD, *Computer Methods for Ordinary Differential Equations and Differential-Algebraic Equations*, SIAM, 1998.
- [3] C.M. BENDER, S. ORSZAG, *Advanced Mathematical Methods for Scientists and Engineers*, McGraw-Hill, International Series in Pure and Applied Mathematics, 1978.
- [4] K.E. BRENNAN, S.L. CAMPBELL AND L.R. PETZOLD, *Numerical Solution to of Initial-Value Problems in Differential-Algebraic Equations*, SIAM Classics in Applied Mathematics, #14, 1996.
- [5] K.D. CLARK AND L.R. PETZOLD, *Numerical Solution to Boundary Value Problems in Differential-Algebraic Systems*, SIAM J. Sci. Stat. Comput., 10 (1989), pp. 915–936.
- [6] M. GOLUBITSKY AND D.G. SCHAEFFER, *Singularities and Groups in Bifurcation Theory, Vol I*, Springer, 1985.
- [7] P.A. GREMAUD, J.V. MATTHEWS AND M. SHEARER, *Similarity solutions for granular materials in hoppers*, in: Nonlinear PDE’s, dynamics, and continuum physics, J. Bona, K. Saxton and R. Saxton Eds., pp. 79–95, Contemporary Mathematics, #255, AMS, 2000.
- [8] A.W. JENIKE, *Gravity flow of bulk solids*, Bulletin No. 108, Utah Eng. Expt. Station, University of Utah, Salt Lake City (1961).
- [9] T.M. KNOWLTON, J.W. CARSON, G.E. KLINZING AND W.C. YANG, *The importance of storage, transfer and collection*, Chem. Eng. Prog., 90 (1994), pp. 44–54.
- [10] E.W. MERROW, *A quantitative assessment of R&D requirements for solids processing technology*, Publication R-3216-DOE/PSSP of the Rand Corporation, 1986.
- [11] R.M. NEDDERMAN, *Static and kinematic of granular materials*, Cambridge University Press, 1992.
- [12] D.G. SCHAEFFER, *Instability in the evolution equations describing incompressible granular flow*, J. Diff. Eq., 66 (1987), pp. 19–50.